Available online at www.sciencedirect.com

ScienceDirect

Procedia Engineering 198 (2017) 758 – 769

Procedia Engineering

www.elsevier.com/locate/procedia

Urban Transitions Conference, Shanghai, September 2016

The influence of building packing densities on flow adjustment and city breathability in urban-like geometries

Lan Chen[a], Jian Hang[a]*, Mats Sandberg[b], Leif Claesson[b], Silvana Di Sabatino[c]

[a]*School of Amopheric Sciences,Sun Yat-sen University,Xingang Xi Road 135, HaiZhu, Guangzhou 510275, China*
[b]*Laboratory of Ventilation and Air Quality, University of Gävle, SE-80176 Gävle, Sweden*
[c]*Department of Physics and Astronomy - DIFA, ALMA MATER STUDIORUM - University of Bologna, Viale Berti Pichat 6/2, 40127 Bologna*

Abstract

City breathability refers to the air exchange process between the flows above and within urban canopy layers (UCL) and that of in-canopy flow, measuring the potential of wind to remove and dilute pollutants, heat and other scalars in a city. Bulk flow parameters such as in-canopy velocity (Uc) and exchange velocity (U_E) have been applied to evaluate the city breathability. Both wind tunnel experiments and computational fluid dynamics (CFD) simulations were used to study the flow adjustment and the variation of city breathability through urban-like models with different building packing densities.

We experimentally studied some 25-row and 15-column aligned cubic building arrays (the building width B=72mm and building heights H=B) in a closed-circuit boundary layer wind tunnel. Effect of building packing densities (λ_p=λ_f=0.11, 0.25, 0.44) on flow adjustment and drag force of each buildings were measured. Wind tunnel data show that wind speed decreases quickly through building arrays due to strong building drag. The first upstream building induces the strongest flow resistance. The flow adjustment length varies slightly with building packing densities. Larger building packing density produces lower drag force by individual buildings and attains smaller velocity in urban canopy layers, which causes weaker city breathability capacity.

In CFD simulations, we performed seven test cases with various building packing densities of λ_p=λ_f=0.0625, 0.11, 0.25, 0.36, 0.44 and 0.56. In the cases of λ_p=λ_f=0.11, 0.25, 0.44, the simulated profiles of velocity and drag force agree with experiment data well. We computed U_c and U_E, which represent horizontal and vertical ventilation capacity respectively. The inlet velocity at 2.5 times building height in the upstream free flow is defined as the reference velocity U_{ref}. Results show that U_E/U_{ref} changes slightly (1.1% to 0.7%) but U_c/U_{ref} significantly decreases from 0.4 to 0.1 as building packing densities rise from 0.0625 to 0.56. Although U_E is induced by both mean flows and turbulent momentum flux across the top surface of urban canopy, vertical turbulent diffusion is found to contribute mostly to U_E.

Peer-review under responsibility of the organizing committee of the Urban Transitions Conference

Keywords: City breahability; Exchange velocity; In-canopy velocity; Flow adjustment; Building packing densiy

* Corresponding author. Tel.: +86 20 8411 0375; fax: +86 20 8411 0375.
E-mail address: hangj3@mail.sysu.edu.cn

Peer-review under responsibility of the organizing committee of the Urban Transitions Conference
doi:10.1016/j.proeng.2017.07.127

1. Introduction

In 2011, more than half of world population (about 3.5 billion) live in cities, and the percentage is predicted to reach 60% (about 5.0 billion) by 2030[1]. The rapid urbanization worldwide and the increasing vehicle emissions in cities have raised environmental concerns on urban air quality[2-4] and urban heat island with respect to the increasing urban energy consumption for summertime cooling [5,6]. Improving urban/city ventilation has been confirmed one of the effective technique in improving urban air quality and reduce urban heat island intensity[7-14].

Thus, recently more ventilation concepts have been applied to measure the capacity of UCL (urban canopy layer) ventilation. It is based on the assumption that the surrounding air is relatively cleaner or cooler, then the air exchange between the external flows and that of the in-canopy flow can bring clear air into cities (inhale effect) and remove pollutants or heat out (exhale effect) — hence the "city breathability". The capacity of city breathability is confirmed with respect to the urban airflow patterns resulting from the interaction between the approaching atmospheric flow and urban morphologies. Horizontal mean flows, vertical mean flows and vertical turbulent diffusions are verified to make significantly contributions. The city breathability (or part of it) can be evaluated by various bulk flow parameters and ventilation indices such as volumetric flow rate, air change rate per hour [24-25, 29-30, 32], purging flow rate, pollutant retention time [10, 34], age of air, ventilation efficiency [25-27, 29], net escape velocity [36], exchange velocity and in-canopy velocity [48-52] etc. Specially, as first originated by Bentham and Britter [48], the concept of exchange velocity (U_E) represents the average velocity of scalar transfer out of or into the UCL at a interface plane (i.e. roof level) between the in-canopy and above-canopy flows, measuring the overall vertical ventilation induced by mean flows and vertical turbulent diffusion. Besides for quantifying the horizontal dilution capacity, the in-canopy velocity (U_C) is defined as constant within the urban canopy layer rather than a velocity profile in street canyons. Then U_E and U_C were later introduced into CFD simulations to successfully estimate the overall capacity of vertical exchange and horizontal dilution in idealized or realistic urban areas [49-52].

According to Belcher et al. [53], the "adjustment region" is downwind of the windward UCL boundaries and below UCL rooftop where the horizontal flow substantially decelerates and a fraction of air is driven out upwardly across UCL roofs (i.e. U_E and U_C changes horizontally). Then it comes into the "canopy interior" region [53] or the "fully-developed region" [32], where a local balance is established between downward transport of momentum by turbulent stresses and removal of momentum by the drag of the canopy elements (i.e. U_E and U_C keep constants).

Defined by Grimmond and Oke [54], the building planar area index λ_p (i.e. the ratio between the planar area of buildings viewed from above and the total floor area) and the frontal area index λ_f (i.e. the ratio of the frontal area of buildings to the total floor area) are usually adopted to quantify urban compactness (Fig. 1). The ratio of street height to width has been proved to affect the street flow pattern. When the buildings space sparsely, there is good ventilation but low land utilization. Denser city layout means a higher land-use but may experience worse UCL ventilation [25-28]. In this context, we aim to attain the influence of building packing densities (λ_f varies from 0.0625 to 0.56) on the capacity of vertical ventilation (U_E) and horizontal dilution (U_C) within and through urban canopy layers. Such researches have been rarely reported.

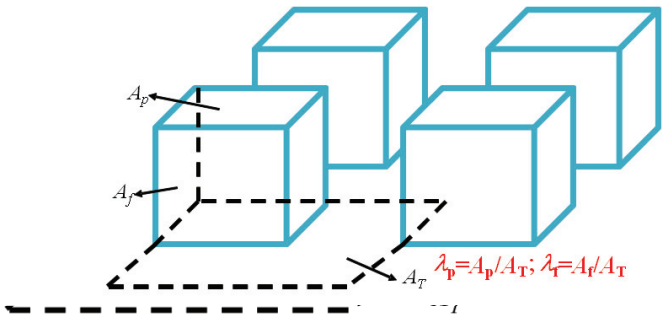

Fig.1 Definition of planar area index λ_p and frontal area index λ_f

2. In-canopy velocity (U_C) and Exchange velocity (U_E)

By considering a constant velocity within the canopy layer, Bentham and Britter [48] firstly deduced the simplified in-canopy velocity (U_C). As presented in Eq. (1) below, the scale of U_C can be determined by the pressure force acting on the building and the drag coefficient. F_p can be calculated by the net pressure surface integral on the frontal and back area of the building unit. C_D is the drag coefficient (a standard value of 1 was chosen), and A_f refers to the frontal area of the building.

$$U_C = \sqrt{\frac{2F_P}{\rho C_D A_f}} \tag{1}$$

The exchange velocity (U_E) is balanced by the drag force exerted on the buildings with regard to the local wall shear stress. Hamlyn and Britter [49] first applied U_E into CFD (Computational Fluid Dynamics) simulations as a ratio of the momentum flux to the difference between the mass flux above and below the top of urban canopy layer (exchange plane).

$$U_E = \frac{\iint (\rho \overline{u'w'} + \rho \bar{u}\bar{w}) dS}{\rho A_C (U_{\text{ref}} - U_C)} \tag{2}$$

The momentum flux in Eq. (2) is evaluated from the Reynolds' shear stresses and the average values of the x and z components of velocities. A_C is the cross area of the exchange plane and U_{ref} is the average velocity at 2.5 times building height in the upstream free flow. Fig.2 gives a brief description of some parameters above.

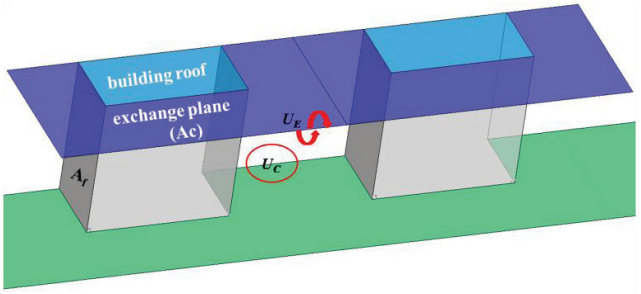

Fig.2 Example of exchange velocity U_E and in-canopy velocity U_C

3. Numerical setup and wind tunnel studies

3.1. Wind tunnel experiments

To study the flow adjustment and evaluate the reliability of CFD simulations, wind tunnel experiments were first carried out in a closed-circuit boundary layer wind tunnel at Laboratory of Ventilation and Air Quality, the University of Gävle, Sweden (Fig. 3). The working test section of wind tunnel is 11 m long, 3 m wide and 1.5 m tall. We investigated 25-row and 15-column square building array with a characteristic dimension of H=B=72mm, where H and B are the height and length/width of the obstacle, corresponding to actual buildings scale of 36m (i.e. the scale ratio is 1:500). By changing the space of buildings, three kinds of building packing densities (λ_p=λ_f=0.11, 0.25, 0.44) were studied. The approaching wind was parallel to the main streets and perpendicular to the secondary streets. We defined the rows of buildings from upstream toward downstream as rows No 1, 2, 3, 4, 5… 25. Then the secondary streets behind building No i were named as canyon No *i*. Point V*i* represents the centre point of the secondary streets (canyons) No *i*. Vertical profiles of velocity *u* (*z*) and turbulence kinetic energy *k (z)* at Points Vi were measured using hotwire anemometers. The measuring frequency was 100 Hz. As we used the measurement

time of 40 s, 60 s and 80 s to perform a time independence study, the measured data changed little. Thus we finally chose 40 s as the measurement time. The drag forces of each building in the middle main column were also measured in wind tunnel experiments. To analyze the cases more easily, we name all building arrays as Case [street width (mm), building packing densities λ_p/λ_f]. So these three wind tunnel studies can be named as case [144, 0.11], case [72, 0.25] and case [36, 0.44]. For case [144, 0.11], it had 20-row array only.

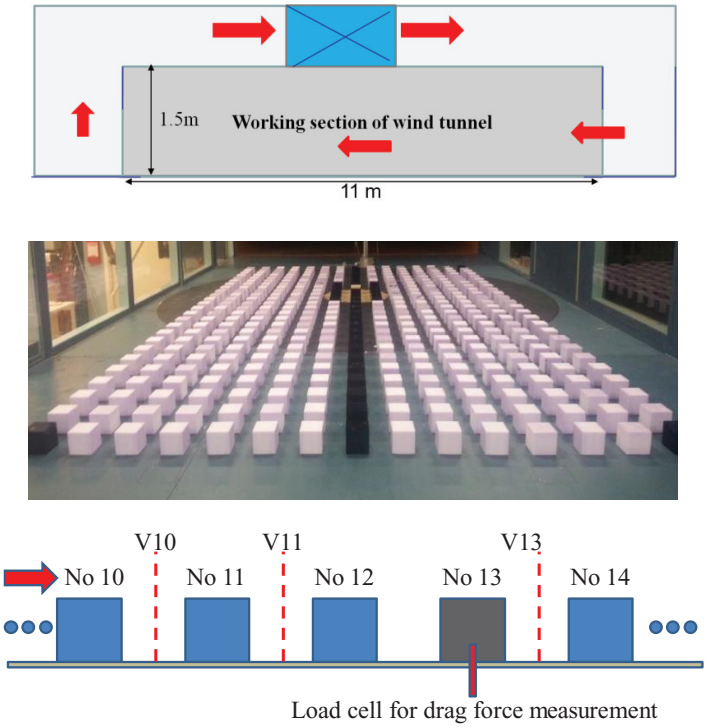

Fig.3 Wind tunnel working section and an example of wind tunnel model

3.2. Numerical setup

As the urban-like square building arrays in wind tunnel experiments was wide enough in the lateral direction, the lateral effects on the flow in the middle main column can be negligible. Therefore, only half of the middle column was considered in CFD simulations to reduce the computational time (Fig.4). Such technique has been widely adopted and confirmed effective in the literature [50,51]. Fig. 4 shows the computational domain and boundary conditions in case [72, 0.25]. The space of building array boundaries to the domain top, domain inlet and domain outlet were set 9.0*H*, 5*H* and 15*H* respectively. Ansys FLUENT with the Standard k-ε model and the RNG k-ε model was used to solve the steady-state flow field [47]. All transport equations were discretized by the second-order upwind scheme. The SIMPLE scheme was used for the pressure and velocity coupling. The total number of hexahedral cells ranged from 180 to 370 million with the minimum grid of below 1mm (i.e. *H*/72mm). Zero normal gradient condition was adopted at the domain top (symmetry), domain outlet (outflow), and two lateral domain boundaries (symmetry). All wall surfaces used no slip boundary condition with standard wall function [47]. We totally made seven simulating cases, as summarized in Table. 1.

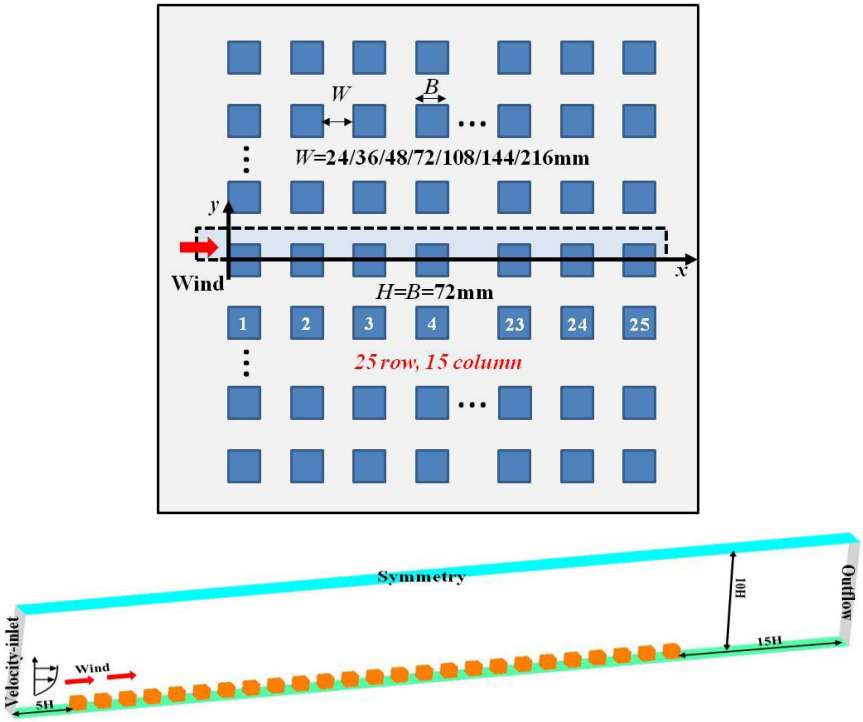

Fig.4 Computational model, domain and boundary conditions in CFD simulations

Table 1 Summary of CFD models investigated

Case name	Cubes scale $H=B$	Obstacles space W	Building packing densities $\lambda p=\lambda f$
[216, 0.0625]	72mm	216mm	0.0625
[144, 0.11]	72mm	144mm	0.11
[108, 0.16]	72mm	108mm	0.16
[72, 0.25]	72mm	72mm	0.25
[48, 0.36]	72mm	48mm	0.36
[36, 0.44]	72mm	24mm	0.44
[24, 0.56]	72mm	24mm	0.56

4. Results and discussion

4.1 Validation of CFD flow modeling evaluated by wind tunnel data

We first used wind tunnel data in the literature [55] to evaluate the reliability of CFD simulations. In wind tunnel experiments [55], a 13-column and 7-row cubic building cluster with the parallel approaching wind was investigated. Building width (B), building height (H) and street width (W) are 15 cm ($\lambda_p=\lambda_f=0.25$, $H/W=1$). Similarly in this CFD validation case, we only considered the middle main column since it was sufficiently wide in the span-wise (lateral) direction. All the other boundary conditions, computational domain and CFD setups are similar with those in subsection 3.2. At the domain inlet, the boundary conditions are defined by the vertical profile of stream-wise

velocity $U_0(z)$ measured in the upstream free flow coupled with the profiles of turbulent kinetic energy k (z) and its dissipation rate (ε) [55].

$$U_0(z) = U_H (z/H)^{0.16} \tag{1a}$$

$$k(z) = u_*^2 / \sqrt{C_\mu} \tag{1b}$$

$$\varepsilon(z) = C_\mu^{3/4} k^{3/2} / (\kappa_v z) \tag{1c}$$

Where u_*=0.24ms^{-1} is the friction velocity, C_μ is 0.09, κ_v =0.4 is von Karman's constant, U_H=3.0ms^{-1} is the undisturbed reference velocity at z=H at the domain inlet.

Fig. 5 shows some example CFD validation profiles using wind tunnel data in the literature [55] of stream-wise velocity $u(z)$ and turbulent kinetic energy $k(z)$ (TKE) at Point V1. For TKE profile, only CFD results with the medium grid are displayed. It verifies that the standard k-ε model performed better in predicting $u(z)$ than the RNG k-ε model. Both models only predicted the shape of $k(z)$ generally well.

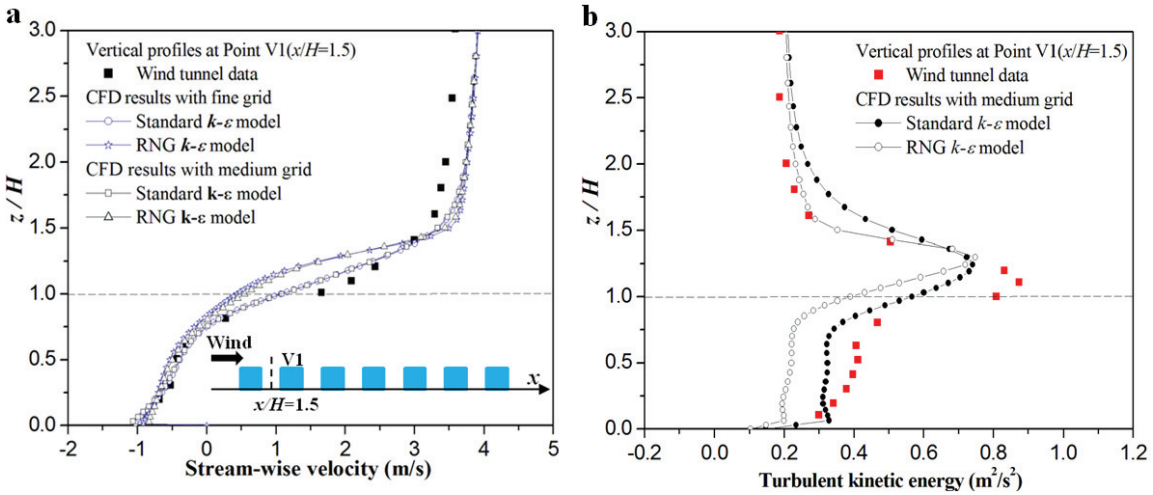

Fig. 5 Example profiles of CFD validation (a)stream-wise velocity at Point V1; (b)turbulent kinetic energy at Point V1 (medium grid only).

Then we adopted wind tunnel data measured by ourselves to evaluate the reliability of CFD simulations. Fig. 6 displays vertical profiles of velocity (or wind speed) u (z) at Point V2 and the horizontal profiles of drag force for each building. Both the standard k-ε model and the RNG k-ε model can predict the velocity profile and drag force distribution basically well, except that the RNG k-ε model did worse in predicting the drag force of building No 2.

Basing on the comparisons in Figs. 5 and 6, the standard k-ε model with the medium grid was selected as the better choice in the following CFD simulations.

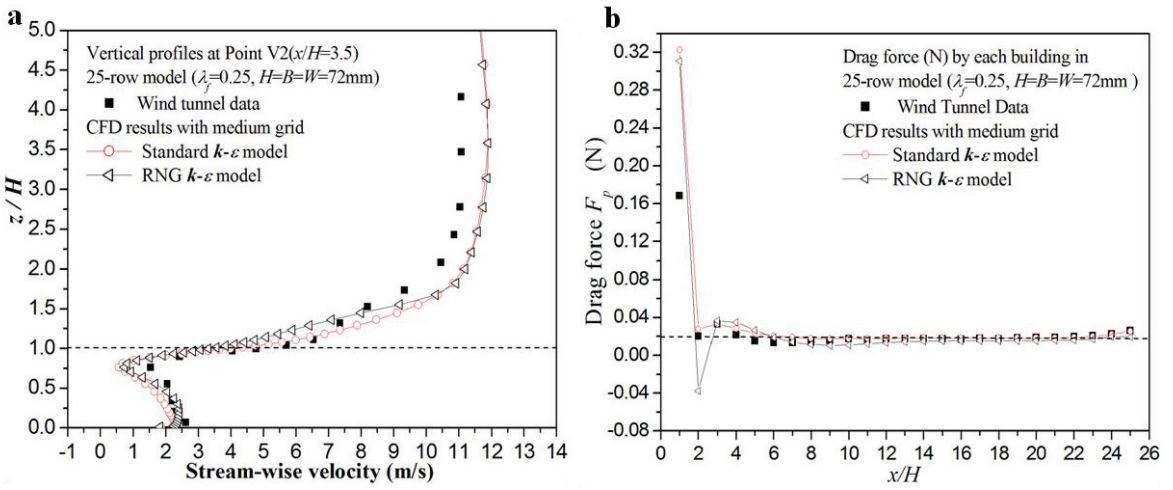

Fig. 6 Example profiles of CFD validation using our wind tunnel data (a) stream-wise velocity at Point V2; (b) drag force for each building.

4.2 Flow adjustment

When wind penetrate into the city through windward openings, the velocity usually decreases as deeper into the city due to the blockage of urban buildings, where is named as the flow adjustment region. After the process of flow adjustment, the macroscopic flow characteristics remain constant and a flow local balance is built up. Then it is considered that the airflow is fully-developed [32]. As an example, Fig. 7 shows the 3D streamline and static pressure in case [72, 0.25]. Blocked and displaced by the first building, the wind was split up, driven over the roof or penetrating into the main street which is parallel to the approaching wind. Three-dimensional vortex structure was observed in the secondary street sheltered by the buildings. Both the horizontal flow in the main street and vertical turbulent diffusion induced by 3D vortexes could bring external clear air into the canyons and help pollutant dilution. Such capacity will be quantified by the in-canopy velocity and exchange velocity respectively.

Fig. 8a-d show horizontal profile of vertical velocity, stream-wise velocity and turbulence kinetic energy alone the main street centerline at z=3mm (i.e. the scale ratio is 1:500) in CFD prediction and drag force by each buildings measured in wind tunnel experiments. Here only three example cases (case [144, 0.11], case [72, 0.25] and case [36, 0.44]) are displayed, represented sparse, medium and compact urban model respectively (building packing densities λ_p=λ_f=0.11, 0.25, 0.44). Vertical velocity, stream-wise velocity and turbulent kinetic energy (TKE) suddenly increase when the wind flows across the windward street opening (at x/H=0) driven by the high pressure difference near first obstacle. Then there is a continuous reduction of velocity and TKE in the followed flow adjustment region.. The velocity and TKE in case [36, 0.44] (the compact one) decrease the most rapidly in adjustment region. After that, a flow balance was established in the “fully-developed region”, where macroscopic flow characteristics remained constant. The value of velocity components and TKE changes following a wave form due to the periodic flow resistances by buildings. The magnitude of stream-wise velocity and TKE in fully-developed region is the greatest in case [144, 0.11] (sparse) and the smallest in case [36, 0.44]. And TKE in case [36, 0.44] decreased almost to zero. Thus, it can be verified that building packing density is the key factor to influence the flow adjustment and urban ventilation capacity through the city model.

The profile of drag force among buildings (Fig. 8d) shows various building packing densities experience different distance of the flow adjustment region and the balanced drag force in the fully developed region. The fully-developed region began from building No 9 in case [144, 0.11],No 6 in case [72, 0.25], and No 4 in case [36, 0.44]. And the drag force by buildings and the corresponding wind speed were obviously the greatest in case [144, 0.11], the medium in case [72, 0.25] and the smallest in case [36, 0.44] (i.e. greater wind speed induce stronger drag force).

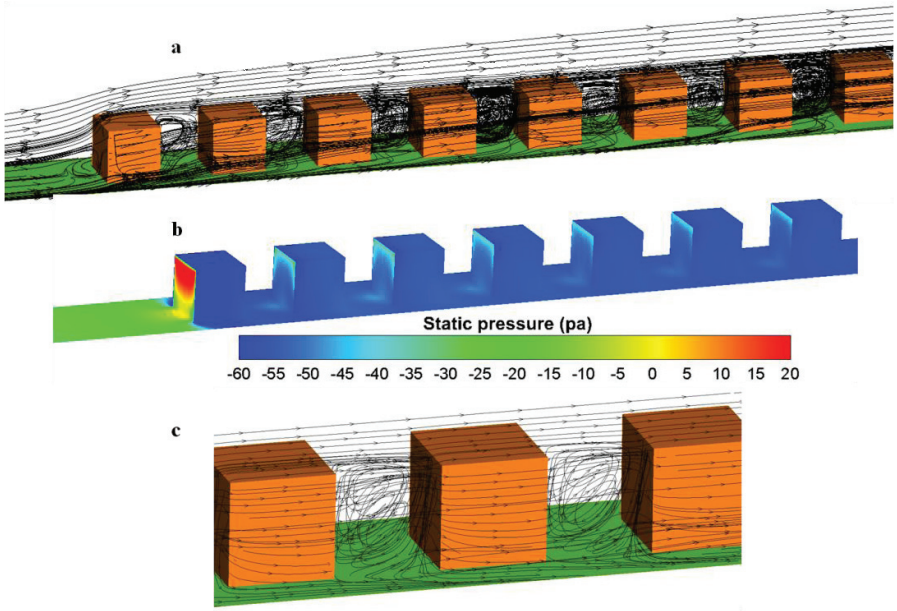

Fig. 7 3D streamline (a) adjustment region, (c) fully-developed region, and (b) static pressure in case [72, 0.25]

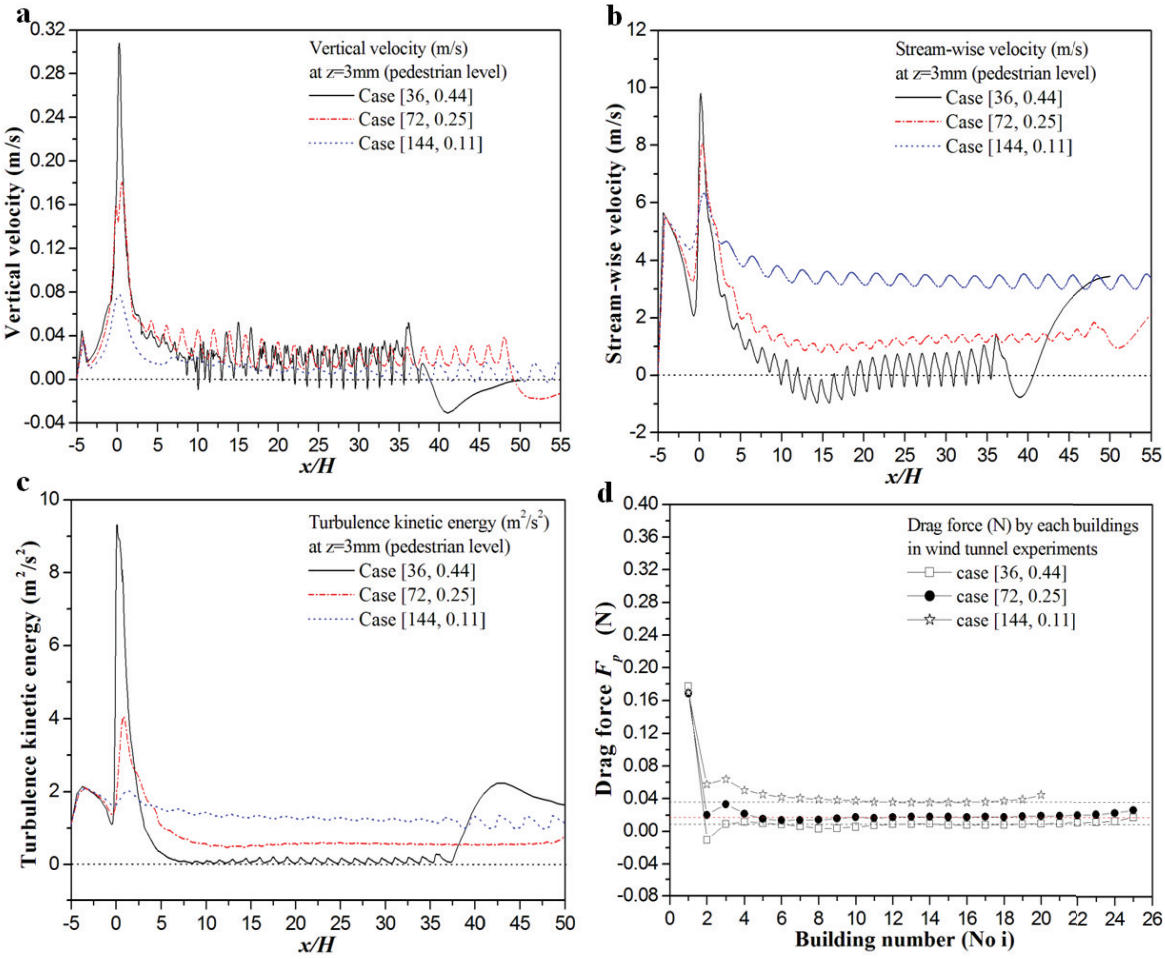

Fig. 8 Horizontal profiles of (a) stream-wise velocity, (b) vertical velocity, (c) TKE, (d) drag force

4.2 In-canopy velocity (U_C) and exchange velocity (U_E)

The in-canopy velocity (U_C) and exchange velocity (U_E) can be used to measure the horizontal diluting capacity and the overall vertical ventilation capacity respectively [48]. Fig. 9 shows the horizontal profiles of U_C and U_E in three example cases (case [36, 0.44], case [72, 0.25] and case [144, 0.11]). Here U_C and U_E are normalized by the reference velocity U_{ref} in the upstream free flow at 2.5 building height. Table.2 summarizes U_C/U_{ref} and U_E/U_{ref} in the fully-developed region of our seven CFD cases, those from CFD simulations by Hamlyn and Britter [49] and corresponding predictions from Bentham and Britter's theoretical model [48]. Similar with the velocity and turbulent kinetic energy, U_E and U_C for each obstacle experience two processes, the adjustment and the quasi-stability state. When calculating the value of U_E/U_{ref}, the turbulent flux in Eq. 2 was substituted by Reynolds' shear stresses.

Fig. 9a displays that the magnitude of exchange velocity U_E/U_{ref} was nearly invariable when building packing densities change. Table 2 further confirms that U_E/U_{ref} in the fully developed region changes slightly from 1.1% to 0.7% with building packing density varying from 0.0625 to 0.56. For low and medium density models (0.0625 to 0.25), U_E/U_{ref} is 1% to 1.1% . The results were very similar with those from Hamlyn and Britter [49], which showed U_E/U_{ref} was around 1% for the $\lambda_p=\lambda_f=0.0625$ and 0.16. While for the compact array ($\lambda_p=\lambda_f=0.36$ to 0.56), our results differ from those of Hamlyn and Britter [49] and Bentham and Britter [48]. For this study, U_E/U_{ref} was 0.72% to 0.88%.In the literature, U_E/U_{ref} for $\lambda_p=\lambda_f=0.44$ was 0.32% in Hamlyn and Britter [49] and 3.8% in Bentham and Britter [48]. It should be noted that, even if U_E changes little, however the overall vertical ventilation will become better when the streets become wider or building packing densities decrease since the overall area of exchange plane A_C (or street roof $A_{roof}=A_T-A_p$ in Fig. 1) for each building unit significantly rises (for example $A_{roof}=3H^2$ for $H/W=1$, $\lambda_p=\lambda_f=0.25$ and $A_{roof}=8H^2$ for $H/W=2$, $\lambda_p=\lambda_f=0.11$).

In-canopy velocity U_C is mainly controlled by the drag force exerting on the building (see Eq. 1) and larger drag force usually represents greater wind speed around the building. As shown in Fig. 8d and Table 2, the drag force and U_C/U_{ref} continuously decrease if building packing density rises from 0.0625 to 0.56, i.e. the values of U_C/U_{ref} are 0.431, 0.312, 0.284, 0.221, 0.176, 0.153 and 0.113 as $\lambda_p=\lambda_f=0.0625$, 0.11, 0.16, 0.25, 0.36, 0.44 and 0.56. Specially the magnitude and variation trend of U_C was similar with those in Hamlyn and Britter [49]. Both Hamlyn and Britter [49] and this study had large discrepancies with the predictions from Bentham and Britter's theoretical model [48]. The predominantly reason was large estimates of friction velocity and in-canopy velocity in Bentham and Britter's model. In their model, momentum exchanges were calculated from ρu^2_* and thus was highly sensitive to the value of friction velocity [49].

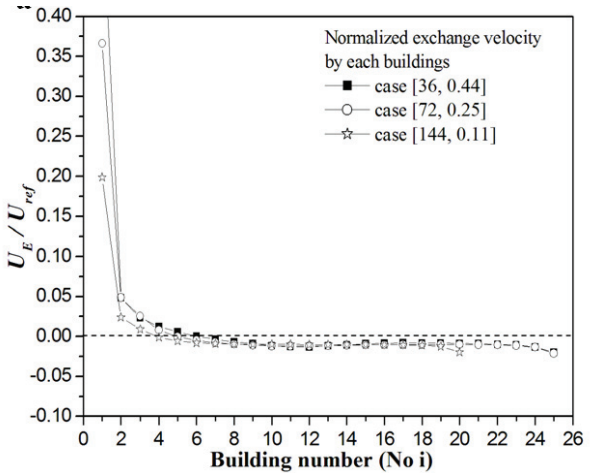

Fig. 9 Horizontal profiles of exchange velocity, in case [36, 0.44], case [72, 0.25] and case [144, 0.11]

Table.2 Comparison of U_C and U_E from this study with results from literatures [48, 49]

Case name		[216, 0.0625]	[144, 0.11]	[108, 0.16]	[72, 0.25]	[48, 0.36]	[36, 0.44]	[24, 0.56]
U_c/U_{ref}	**This study**	**0.431**	**0.312**	**0.284**	**0.221**	**0.176**	**0.153**	**0.113**
	Hamlyn-CFD	0.433		0.373			0.177	
	Bentham-theoretical	0.584		0.534	0.406		0.240	
U_E/U_{ref}	**This study**	**0.0106**	**0.0102**	**0.0098**	**0.0103**	**0.0088**	**0.0083**	**0.0072**
	Hamlyn-CFD	0.0109		0.0094			0.0032	
	Bentham-theoretical	0.037	0.042	0.054	0.036		0.038	

5. Conclusion

The flow adjustment and the variation of in-canopy velocity and exchange velocity in urban-like models with different building packing densities were investigated using the wind tunnel experiments and CFD simulations with the standard k-ε turbulent model. The CFD flow modelling was validated well by wind tunnel data. It is found that, larger building packing density (or narrower streets) experience a quicker wind reduction, shorter distance of flow adjustment region, smaller velocity components, TKE and in-canopy velocity (U_C) in fully-developed region.

The in-canopy velocity (U_C) and exchange velocity (U_E) are normalized by the reference velocity at the building height of 2.5times in the upwards free flow (U_{ref}).The CFD results show that U_E/U_{ref} changes slightly from 1.1% to 0.7% with building packing density rising from 0.0625 to 0.56 while Uc/U_{ref} significantly decreases from 0.43 to 0.11. The horizontal diluting capacity is considered to be significantly weakened as the packing density increases. Though the value of U_E is insensitive to the building packing density, the overall vertical ventilation capacity will be strengthened by wider streets or smaller building packing density considering the total area of exchange plane increases with the decreasing building packing density.

Acknowledgements

This study was financially supported by the National Natural Science Foundation of China (No 51478486) and special fund of Key Laboratory of Eco Planning & Green Building, Ministry of Education (Tsinghua University), China (No 2013U-5).

References

[1] J. Van der Geer, J.A.J. Hanraads, R.A. Lupton, The art of writing a scientific article, J. Sci. Commun. 163 (2000) 51–59.
[2] W. Strunk Jr., E.B. White, The Elements of Style, third ed., Macmillan, New York, 1979.
[3] G.R. Mettam, L.B. Adams, How to prepare an electronic version of your article, in: B.S. Jones, R.Z. Smith (Eds.), Introduction to the Electronic Age, E-Publishing Inc., New York, 1999, pp. 281–304.

[1] Population division of the Department of Economic and Social Affairs of the United Nations Secretariat. New York: United Nations: World Urbanization Prospects: The 2007 Revision. 2011.
[2] Fenger J, Urban air quality, Atmos Environ. 33 (1999) 4877-4900.
[3] Luo Z, Li Y, Nazaroff WW, Intake fraction of nonreactive motor vehicle exhaust in Hong Kong, Atmos Environ. 44 (2010) 1913-1918.
[4] W. Ji, B. Zhao, Estimating mortality derived from indoor exposure to particles of outdoor origin, PLOS. ONE. 10 (2015) e0124238.
[5] Kolokotroni M, Giannitsaris I, Watkins R, The effect of the London urban heat island on building summer cooling demand and night ventilation strategies, Solar Energy. 80 (2006) 383-392.
[6] Srebric, J., Heidarinejad, M., Liu, JY, Building neighbourhood emerging properties and their impacts on multi-scale modelling of building energy and airflows, Build Environ. 91 (2015) 246-262.
[7] Deng Q, He G, Lu C, Liu W, Urban Ventilation - A New Concept and Lumped Model, Int J Vent. 11(2012) 131-140.
[8] Zhang Y, Gu Z, Air quality by urban design, Nat Geosci. 6(2013) 506-506.

[9] Ng W, Chau C, A modeling investigation of the impact of street and building configurations on personal air pollutant exposure in isolated deep urban canyons, Sci Total Environ. (2014) 468-469 429-48.
[10] Bady M, Kato S, Huang H, Towards the application of indoor ventilation efficiency indices to evaluate the air quality of urban areas, Build Environ. 43 (2008) 1991-2004.
[11] Hang J, Luo Z, Sandberg M, Gong J, Natural ventilation assessment in typical open and semi-open urban environments under various wind directions, Build Environ. 70 (2013) 318-333.
[12] Ng E, Policies and technical guidelines for urban planning of high-density cities - air ventilation assessment (AVA) of Hong Kong, Build Environ. 44(2009) 1478-1488.
[13] Yuan C, Ng E, Norford LK, Improving air quality in high-density cities by understanding the relationship between air pollutant dispersion and urban morphologies, Building Environ. 71 (2014) 245-258.
[14] Yang F, Qian F, Lau S SY, Urban form and density as indicators for summertime outdoor ventilation potential: A case study on high-rise housing in Shanghai, Build Environ. 70 (2013) 122-137.
[15] Britter RE, Hanna SR, Flow and dispersion in urban areas, Annu Rev Fluid Mech. 35 (2003) 469-496.
[16] Fernando HJS, Zajic D, Di Sabatino S, Dimitrova R, Hedquist B, Dallman A, Flow, turbulence, and pollutant dispersion in urban atmospheres, Phys Fluids. 22(2010) 051301.
[17] Di Sabatino S., R. Buccolieri, P. Salizzoni, Recent advancements in numerical modelling of flow and dispersion in urban areas: a short review, Int. J. Environ. Pollut. 52(2013) 172-191.
[18] Meroney, R.N., Ten questions concerning hybrid computational/physical model simulation of wind flow in the built environment, Build. Environ. 96 (2016) 12-21.
[19] Blocken B., Computational fluid dynamics for urban physics: importance, scales, possibilities, limitations and ten tips and tricks towards accurate and reliable simulations, Build. Environ. 91(2015) 219-245.
[20] Li X.X., C.H. Liu, D.Y.C. Leung, K.M. Lam, Recent progress in CFD modelling of wind field and pollutant transport in street canyons, Atmos. Environ. 40(2006) 5640-5658.
[21] Ashie Y, Kono T, Urban-scale CFD analysis in support of a climate-sensitive design for the Tokyo Bay area, Int J Climatol. 31(2011) 174-188.
[22] Meroney, R.N., Pavegeau, M., Rafailidis, S., Schatzmann, M, Study of line source characteristics for 2-D physical modelling of pollutant dispersion in street canyons, J. Wind. Eng. Ind. Aerodyn. 62 (1996) 37–56.
[23] Li XX, Liu CH, Leung DYC, Numerical investigation of pollutant transport characteristics inside deep urban street canyons, Atmos Environ. 43(2009) 2410-2418.
[24] Liu CH, Leung DYC, Barth MC, On the prediction of air and pollutant exchange rates in street canyons of different aspect ratio using large-eddy simulation, Atmos Environ. 39 (2005) 1567-1574.
[25] Hang J, Li Y, Age of air and air exchange efficiency in high-rise urban areas, Atmos Environ. 45(2011) 5572-5585.
[26] Ramponi, R., Blocken, B., de Coo, L.B., Janssen, W.D., CFD simulation of outdoor ventilation of generic urban configurations with different urban densities and equal and unequal street widths, Build. Environ. 92 (2015) 152-166.
[27] Buccolieri R, Sandberg M, Di Sabatino S, City breathability and its link to pollutant concentration distribution within urban-like geometries, Atmos Environ. 44 (2010) 1894-1903.
[28] Chang, C.H., Meroney, R.N., 2003. Concentration and flow distributions in urban street canyons: wind tunnel and computational data. J. Wind. Eng. Ind. Aerodn. 91, 1141-1154.
[29] Hang J, Sandberg M, Li Y, Age of air and air exchange efficiency in idealized city models, Build Environ. 44(2009) 1714-1723.
[30] Lin M, Hang J, Li YG, Luo ZW, Sandberg M, Quantitative ventilation assessments of idealized urban canopy layers with various urban layouts and the same building packing density, Build Environ. 79 (2014) 152-167.
[31] Moonen P, Dorer V, Carmeliet J, Effect of flow unsteadiness on the mean wind flow pattern in an idealized urban environment, J Wind Eng Ind Aerodyn. 104 (2012) 389-396.
[32] Kanda, M., Large-eddy simulations on the effects of surface geometry of building arrays on turbulent organized structures, Boundary-lay, Meteorol. 18 (2006) 151-168.
[33] Gu ZL, Zhang YW, Cheng Y, Lee SC, Effect of uneven building layout on air flow and pollutant dispersion in non-uniform street canyons, Build Environ. 46 (2011) 2657-65.
[34] Hang J, Li Y, Sandberg M, Buccolieri R, Di Sabatino S, The influence of building height variability on pollutant dispersion and pedestrian ventilation in idealized high-rise urban areas, Build Environ. 56 (2012) 346-360.
[35] Garcia-Sanchez C, Philips DA, Gorle C, Quantifying inflow uncertainties for CFD simulations of the flow in downtown Oklahoma City, Build Environ. 78 (2014) 118-129.
[36] Hang J, Wang Q, Chen XY, Sandberg M, Zhu W, Buccolieri R, Di Sabatino S, City breathability in medium density urban-like geometries evaluated through the pollutant transport rate and the net escape velocity, Building and Environment. 94 (2015) 166-182.
[37] Gromke, C., Blocken, B., Influence of avenue-trees on air quality at the urban neighborhood scale. Part I: Quality assurance studies and turbulent Schmidt number analysis for RANS CFD simulations, Environ. Pollut. 196 (2015) 214- 223.
[38] Gromke, C., Blocken, B., Influence of avenue-trees on air quality at the urban neighborhood scale. Part II: Traffic pollutant concentrations at pedestrian level, Environmental Pollution. 196 (2015) 176-184.
[39] Allegrini J, Dorer V, Carmeliet J, Buoyant flows in street canyons: Validation of CFD simulations with wind tunnel measurements, Build Environ. 72 (2014) 63-74.
[40] Allegrini J, Dorer V, Carmeliet J, Wind tunnel measurements of buoyant flows in street canyons, Build Environ. 59 (2013) 315-326.
[41] Cai X, Effects of differential wall heating in street canyons on dispersion and ventilation characteristics of a passive scalar, Atmos Environ. 51 (2012) 268-277.
[42] Dallman A, Magnusson S, Britter R, et al, Conditions for thermal circulation in urban street canyons, Building & Environment. 80 (2014) 184-191.
[43] Yang X, Li Y, Yang L, Predicting and understanding temporal 3D exterior surface temperature distribution in an ideal courtyard, Build Environ. 57 (2012) 38-48.

[44] Cui, P.Y. , Li, Z. , Tao, W.Q., Wind-tunnel measurements for thermal effects on the air flow and pollutant dispersion through different scale urban areas. Build. Environ. 97 (2016) 137-151.
[45] Luo Z, Li Y, Passive urban ventilation by combined buoyancy-driven slope flow and wall flow: Parametric CFD studies on idealized city models, Atmos Environ. 45 (2011) 5946-5956.
[46] Wang, X.X., Li, Y.G., Predicting urban heat island circulation using CFD, Build. Environ. 99 (2016) 82-97.
[47] Nazarian, N., Kleissl, J., Realistic solar heating in urban areas: Air exchange and street-canyon ventilation, Build. Environ. 95 (2016) 75-93.
[48] Bentham T, Britter RE, Spatially averaged flow within obstacle arrays, Atmos Environ. 37 (2003) 2037-2043.
[49] Hamlyn D, Britter R, A numerical study of the flow field and exchange processes within a canopy of urban-type roughness, Atmos Environ. 39 (2005) 3243-3254.
[50] Di Sabatino, S., Buccolieri, R., Pulvirenti, B., Bitter, R., Simulations of pollutant dispersion within idealised urban-type geometries with CFD and integral models, Atmos. Environ. 41 (2007) 8316-8329.
[51] Solazzo E, Britter RE, Transfer processes on a simulated urban street canyon, Bound-Layer Meteorol 124 (2007) 43–60.
[52] Panagiotou I, Neophytou MKA, Hamlyn D, Britter RE, City breathability as quantified by the exchange velocity and its spatial variation in real inhomogeneous urban geometries: An example from central London urban area, Sci Total Environ. 442 (2013) 466-477.
[53] Belcher S, Jerram N, Hunt J, Adjustment of turbulent boundary layer to a canopy of roughness elements, J Fluid Mech. 488 (2003) 369-368.
[54] Grimmond CSB, Oke TR, Aerodynamic properties of urban areas derived, from analysis of surface form, J Appl Meteorol. 38(1999) 1262-1292.
[55] Lien FS, Yee E. Numerical modelling of the turbulent flow developing within and over a 3-D building array, part I: A high-resolution Reynolds-averaged Navier-Stokes approach, Boundary-layer Meteorol. 112 (2004) 427-466.